Reversible Melting in Polymer Crystals Detected by Temperature-Modulated Differential Scanning Calorimetry

Iwao Okazaki[†] and Bernhard Wunderlich*

Department of Chemistry, The University of Tennessee, Knoxville, Tennessee 37996-1600, and Chemical and Analytical Sciences Division, Oak Ridge National Laboratory, Oak Ridge, Tennessee 37831-6197

Received October 17, 1996[⊗]

ABSTRACT: A small amount of locally reversible melting and crystallization in poly(ethylene terephthalate) (PET) has been detected by temperature-modulated differential scanning calorimetry (TMDSC). Extended-time TMDSC was used in the quasi-isothermal mode. Studied were melt-crystallized, quenched, and a biaxially-oriented film of PET in temperature steps of 2 K from 320 to 560 K. The integral of the endothermic and exothermic latent heat contributions to the reversible melting and crystallization is less than 10% of the total heat of fusion and decreases further with time over many hours. The new observations support the concept that "molecular nucleation" is the reversible and rate-determining step in crystallization. On TMDSC, partially-melted chains remain on the surface of higher-melting crystals to permit crystallization during the cooling cycle without supercooling.

Introduction

Melting and crystallization have been a subject of continued interest in the field of macromolecules. A first extensive discussion can be found already in the treatise of Stuart.[1] A summary of the available information up to 1980 can be found in ref 2. Furthermore, unsolved problems of melting and crystallization were addressed in two discussion meetings that set milestones of progress. One was sponsored by the Faraday Society[3] (Cambridge, 1979) and the other by NATO[4] (Mons, 1992). Still, a number of questions concerning the melting and crystallization equilibrium of polymers remain open. Using the nomenclature derived by Ubbelohde,[5] the structure of the melt of flexible molecules, such as macromolecules, is *anticrystalline* because of conformational isomerization[6] introduced on melting. Crystals of rigid and spherical motifs, in contrast, are often *quasi-crystalline* in their liquid state, i.e., their structures can be related to the crystal structure and its lattice.[5] The anticrystalline structure of the liquid state is at the root of the generally observed irreversibility of polymer melting.[2] The research of this paper offers support to the suggestion that there exists reversibility of polymer melting, but only on a molecular or submolecular scale. As soon as a molecule is completely melted, reversibility is lost due to the need for *molecular nucleation*, a rate-determining step with a free-enthalpy barrier for the beginning of crystallization of a molecule or, at higher supercooling, part of a molecule on the surface of a crystal.[2,7,8] Before melting of a molecule is complete, i.e., a part larger or equal to a molecular nucleus remains crystallized, melting and crystallization are shown in this paper to be reversible within a fraction of a kelvin. For the understanding of crystallization of macromolecules, molecular nucleation must be considered in addition to crystal nucleation. Crystal nucleation is always the first step of any crystallization, but it can be easily avoided experimentally by the addition of nuclei.[2] Molecular nucleation, in contrast, can only be affected by changing the molecular conformation in the melt or solution.

The studies of this paper are based on temperature-modulated differential scanning calorimetry (TMDSC), a new thermal analysis technique.[9−11] Specifically, a calorimeter of the heat-flux type, the Modulated DSC of TA Instruments, MDSC, was used to study the melting region of a series of differently crystallized poly(ethylene terephthalate)s (PET). The modulation of the temperature in MDSC consists of a sinusoidal oscillation, superimposed on a constant, underlying heating rate $dT_b/dt = \langle q \rangle$ of the environment of the twin calorimeters (heater or block temperature, T_b). At steady state, the sample temperature, $T_s(t)$, is given by[12]

$$T_s(t) = T_o + \langle q \rangle t - \langle q \rangle \frac{C_s}{K} + A \sin(\omega t - \epsilon) \qquad (1)$$

where T_o is the temperature at the start of the experiment, C_s is the heat capacity of the sample calorimeter (sample + pan), K is Newton's law constant for heat flux governed by a temperature difference,[13] A is the maximum amplitude of the sample-temperature modulation of typically 1.0 K, ω is the angular modulation frequency $2\pi/p$, with p being the modulation period in seconds, typically 60 s, and ϵ is the phase shift relative to the temperature oscillation of the heater (block). An analogous equation holds for the reference temperature, T_r (maximum amplitude A_r and phase shift ϕ). The reference calorimeter usually consists of an empty pan. The temperature difference, $\Delta T = T_r - T_s$ (maximum amplitude A_Δ and phase shift δ) is then proportional to the heat flow (HF). The modulation amplitude of the block temperature is regulated so that the sample-temperature amplitude, A, achieves the value chosen for the experiment (i.e., 1.0 K). A full description of the method is given in ref 12. It relies on the linearity of the Fourier equation of heat flux, negligible temperature gradient within the sample, and achievement of steady state.[14] In the present experiments, the quasi-isothermal method is employed which involves a series of measurements at various constant temperatures, T_o, without an underlying heating rate ($\langle q \rangle = 0$, see eq 1).[15] This method allows extended-time experiments, so that one can separate the slower irreversible crystal rearrangement, annealing, and recrystallization processes, common in polymer crystal melting, from the reversible heat capacity and any reversible melting and crystallization.

The heat flow that follows the temperature modulation measures the "reversing" heat capacity. It is

[†] On leave from Toray Industries, Inc., Otsu, Shiga 520, Japan.
[⊗] Abstract published in *Advance ACS Abstracts,* March 1, 1997.

S0024-9297(96)01539-2 CCC: $14.00

determined by evaluation of the maximum amplitude of the temperature difference, A_Δ, by a partial Fourier analysis:[12]

$$mc_p = \frac{A_\Delta}{A}\sqrt{\left(\frac{K}{\omega}\right)^2 + C'^2} = \frac{A_{HF}}{A}K' \qquad (2)$$

where A and ω are parameters set at the beginning of the experiment, and C' is the heat capacity of the empty reference pan of mass identical to that of the empty sample pan. Newton's law calibration constant K is independent of modulation frequency and reference heat capacity. The "total heat capacity", consisting of reversible *and* irreversible contributions, can either be determined from a standard DSC measurement or be extracted from TMDSC with an underlying heating rate $\langle q \rangle$:

$$mc_p \approx \frac{K\langle \Delta T \rangle}{\langle q \rangle} = \frac{K''\langle HF \rangle}{\langle q \rangle} \qquad (3)$$

For a standard DSC the values in angular brackets are the measured and chosen values of the experiment; in TMDSC they are the sliding averages over one modulation period ($\pm^1/_2 p$). This averaging eliminates the modulation effect. In case the heat capacity is totally reversible, eqs 2 and 3 give the same results.

Many first-order melting and disordering transitions are sufficiently fast, so that their kinetics can be neglected.[2] For transitions with low enthalpy changes over a wider temperature range it may be possible to keep steady state during melting. Then, the transition can be extracted from the "apparent heat capacity" by subtracting the appropriate baseline of the known, transition-free heat capacity which is available, for example, from the ATHAS Data Bank.[16] For sufficiently small apparent heat capacities, steady state may even be reached in TMDSC.

A quite different behavior is often observed for semicrystalline polymers. During melting they may recrystallize, anneal, and perfect. These processes occur usually via nonequilibrium paths.[2,13,14] If these processes are far from equilibrium or sufficiently fast, they may not be modulated and are observed as fully irreversible phenomena in TMDSC; i.e., they show only in the total heat flow of eq 3 and give no contribution to the reversing heat capacity of eq 2. A typical example is the cold crystallization of poly(ethylene terephthalate), shown as Figure 10, below. Even if steady state is lost, however, the total areas of heat flow of the transition peaks are linear.[17]

For the case where the heating cycle of TMDSC can achieve melting under zero-entropy-production conditions[18] and the supercooling of the just melted polymer needed for crystallization is more than twice the modulation amplitude ($2A$), one would expect an endotherm during the first positive modulation that exceeds the melting temperature, not to be followed by a corresponding crystallization exotherm on cooling. In quasi-isothermal experiments any initial loss of steady state due to excessive heat of fusion would die down after a few cycles. As a result, one expects after the initial melting a response solely due to the heat capacity given by eq 2 for the fully or partially melted sample. If one finds additional contributions to give a higher apparent heat capacity, these must originate from reversible melting and crystallizations, as will be illustrated in this paper for the first time.

Experimental Details

Instrumentation, Calibration, and Measurements. A commercial Thermal Analyst 2920 MDSC system from TA Instruments Inc. was used for the measurements on poly(ethylene terephthalate). Dry N_2 gas with a flow rate of 30 mL/min was purged through the sample. Cooling was accomplished with the refrigerated cooling system (RCS) to 193 K. The sample mass was about 5.0 mg. For the calibration of the heat-flow amplitude, 24.9 mg of sapphire was used.[19] The pan weights were always about 23 mg and matched on the sample and reference sides to approach close symmetry of the calorimeters. The modulation amplitude of the sample temperature, A, was chosen such that steady state could be maintained within the changes in heating rates due to modulation. Detailed graphs for the modulation limits were published earlier.[15]

The major experiments were carried out quasi-isothermally. Separate experiments were carried out every 2 K over the temperature range of 320 to 560 K. The amplitude A was set to 1.0 K, coupled to periods of 60 s, to give the maximum heating rates of ±6.3 K/min. Crystallinities and the total heat capacity were also derived from standard DSC measurements at a heating rate of 10 K/min.

Sample Description. The PET samples were of industrial type (Toray Industries, Inc.) with a viscosity-average molar mass of 18 000 Da (intrinsic viscosity of 0.615 dL/g in *o*-chlorophenol). The amorphous PET was prepared by quenching with liquid nitrogen. Data bank values for the glass transition temperature, T_g, and the increase in heat capacity at T_g, ΔC_p, are 342 K and 77.8 J K^{-1} mol^{-1}, respectively. The equilibrium melting temperature, T_m, and the heat of fusion at T_m, ΔH_f, are 553 K and 26.9 kJ mol^{-1}, respectively. The mass of the repeating unit is 192.2 Da.[16] Semicrystalline poly(ethylene terephthalate) was prepared by melt crystallization (cooling from the liquid state) with a cooling rate of 5−20 K min^{-1}. The crystallinity of samples grown from the melt with the slower cooling rates was about 44%. Biaxially oriented films of PET were made of the resin. PET was dried, and then a practically amorphous sheet was prepared. This was stretched in two orthogonal directions to the extension ratio 3.5 × 3.5 at 368 K and then further crystallized at 473 K.

Data Treatment. The recording and deconvolution of the signals are done by the software of the MDSC. Details were given earlier,[12] and a modeling scheme of the deconvolution has been presented.[20] A standard quasi-isothermal run took 20 min, of which the last 10 min were used for heat capacity data collection. An estimate of the heat capacity of the sample calorimeter, C_s ($=mc_p + C'$, *i.e.*, sample + pan heat capacities), and Newton's law constant, K, was made. The ratio C_s/K outside the melting range is less than 1.0 s. It determines the instrument lag for a given heating rate. The maximum lag in heat capacity due to the calorimeter operating at heating rate q with a continuous change in heat capacity of the sample, C_s, was derived earlier and is outside of the error limit for the here reported heat capacities in the transition region.[14]

Results

Figure 1 shows an example of the modulated heat flow and the deconvoluted maximum amplitude of this heat flow as a function of time for the quasi-isothermal experiment at 450 K, a temperature outside the melting and glass transition ranges. It takes about 6−8 min to approach steady state for the maximum heat-flow amplitude, A_{HF}. Note, however, that the deconvolution makes use of data extending 1.5 modulation periods p in either direction of the point under consideration. The modulated heat flow $HF(t)$ has, thus, reached steady state somewhat earlier.

Figure 2a shows the modulated heat flow at 523 K, close to the temperature of maximum melting. The maximum amplitude of the heat flow converges again quickly to steady state. A closer inspection reveals, however, that the maximum amplitude decreases slightly after reaching steady state. This slow decrease can be

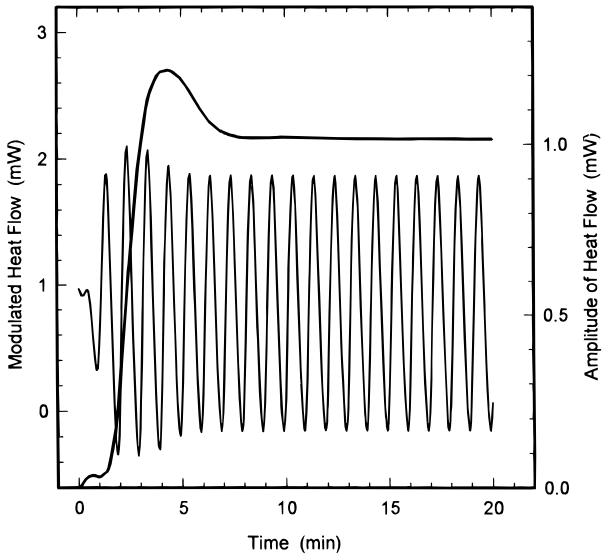

Figure 1. Modulated heat flow and amplitude of heat flow against time for the quasi-isothermal at 450 K in the step-heating experiment. This is an example outside of the melting and glass transition ranges for melt-crystallized PET.

seen better from the extended run at 522 K shown in Figure 2b. Again, even after 2 h a fully reversible heat capacity has not been reached. Estimates of the time needed to reach a fully reversible heat capacity are 20 h or more.

Figure 3 shows plots of the modulated heat flow vs the modulated temperature for the first and second 10 min of the quasi-isothermal experiments shown in Figures 1 and 2a. Approach to steady state and accomplished steady state are illustrated by the perfection of the Lissajous figures. Even the small remaining excess of melting documented in Figure 2b can be seen in the bottom right figure from the slowly decreasing amplitude of the heat flow.

In Figure 4 the times to decrease the reversing heat capacity to within 5, 3, and 1% of the value at 20 min are shown for melt-crystallized PET. The sample reaches 1% in less than 10 min, except in the major melting region (500−550 K). In this melting region it takes up to 14 min to converge to within 1% of the 20 min value. A much smaller effect is seen on cooling from the melt, as is shown in Figure 5. A change in the time to reach steady state after a temperature change is also seen in the glass transition region (330−370 K). A shallow maximum is superimposed on the otherwise decreasing trend for time to reach steady state at increasing temperature. On cooling, the maximum is reached at the glass transition temperature (Figure 5), on heating, at the beginning of the glass transition region (Figure 4).

The heat capacities of both a standard DSC and a quasi-isothermal analysis in 2 K steps are shown in Figure 6 (thick line and open circles, respectively). The heat capacity agrees well with the expected values from the ATHAS data bank,[16] based on adiabatic calorimetry and standard DSC. The glass transition is seen for both total and reversing heat capacities with practically no hysteresis, as is expected for semicrystalline PET.[21] Either a gradual loss of the rigid amorphous fraction or early minor reversible melting seems to occur above the glass transition. Eventually, the reversing (and total) heat capacity crosses the calculated semicrystalline heat capacity at about 430 K, the beginning of the increase into the major melting peak. Most of the DSC melting peak is irreversible; i.e., the quasi-isothermal

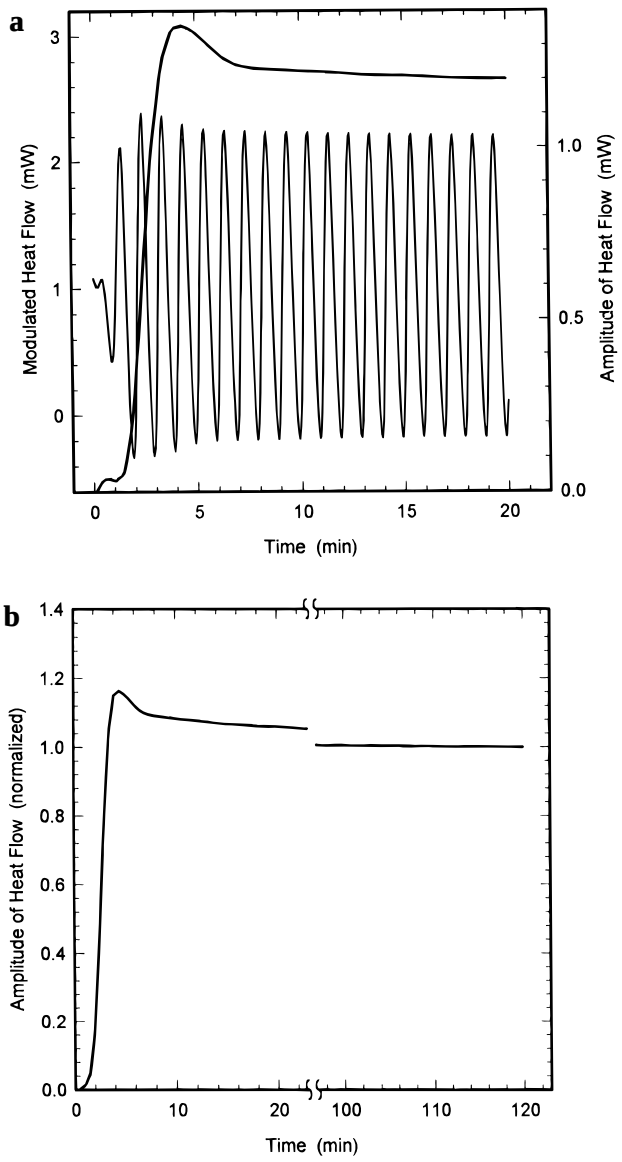

Figure 2. (a) Same as Figure 1 but in the melting region at 523 K. (b) Amplitude of heat flow against time extended to 2 h in the melting region at 522 K.

measurement shows only a small increase beyond the heat capacity of the semicrystalline sample. The extension of the reversible melting and crystallization to higher temperatures than for the irreversible standard DSC is due to annealing, occurring during the sequences of 20 min of quasi-isothermal measurements. The integral of the amplitudes of the quasi-isothermal experiment with a normal baseline is 1.71 kJ/mol, which corresponds to only 6.4% of the equilibrium heat of fusion of 26.9 kJ/mol of the data bank. The crystallinity of the melt-crystallized PET by standard DSC is 44%.

To check on the remaining crystallinity after quasi-isothermal experiments, the samples were quickly cooled and measured by standard DSC. Figure 7 summarizes the DSC traces. Differences occur after the marked temperatures of the quasi-isothermal experiment. Clearly seen are annealing peaks a few kelvins above the annealing temperature.[2] The main melting peak has not shifted relative to the initial sample shown in Figure 6. To prove that the observed changes of Figure 7 are not due to the cooling that preceded the DSC run, two runs were made without cooling and are shown in Figure 8, superimposed on the corresponding curves of Figure 7. The initial approach of steady state is seen in the almost vertical line that reaches the DSC

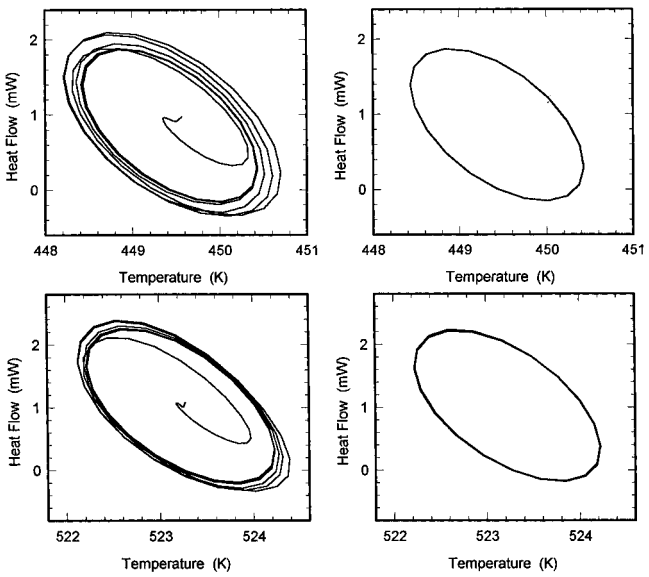

Figure 3. Lissajous figures indicating modulated heat flow versus modulated temperature. (left upper) at 450 K, first 10 min; (right upper) at 450 K, second 10 min; (left lower) at 523 K, first 10 min, (right lower) at 523 K, second 10 min. All are for melt-crystallized PET.

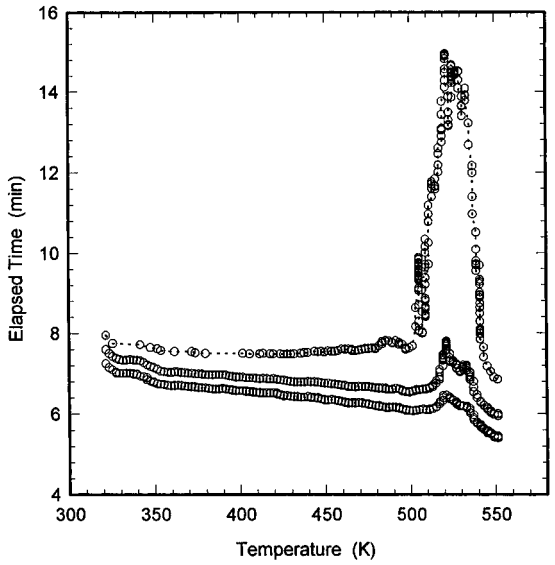

Figure 4. Elapsed time to approach the 20 min value of the maximum amplitude of heat flow for quasi-isothermal TMDSC of melt-crystallized PET. Open circles from top to bottom 1%, 3%, and 5% convergence.

curve of Figure 7 a few kelvins above T_o of the quasi-isothermal experiments. Negligible differences occur thereafter.

The reversing heat capacity for PET measured by the quasi-isothermal TMDSC on cooling from the melt is shown in Figure 9 by the filled circles. For comparison the reversing heat capacity of Figure 6 is shown by the open circles. The crystallinity of the PET after cooling through all the steps of the quasi-isothermal experiment was 49% when measured by standard DSC on reheating. The integral value on the quasi-isothermal step-cooling run above a liquid baseline is 0.14 kJ/mol.

The reversing heat capacity for melt-quenched, amorphous PET by the quasi-isothermal measurement is shown in Figure 10 (filled circles). Again, the reversing heat capacity of Figure 6 is shown for comparison by the open circles. The glass transition at about 350 K is followed at about 375 K by cold crystallization. No effect outside the decrease in heat capacity due to crystallization is seen on cold crystallization. The crystallization is fully irreversible. The integral value of the reversing heat capacity of the melt-quenched sample above the baseline is 2.83 kJ/mol; i.e., it results in a crystallinity of 10.5%. The crystallinity of the sample after cold crystallization by standard DSC is 40%.

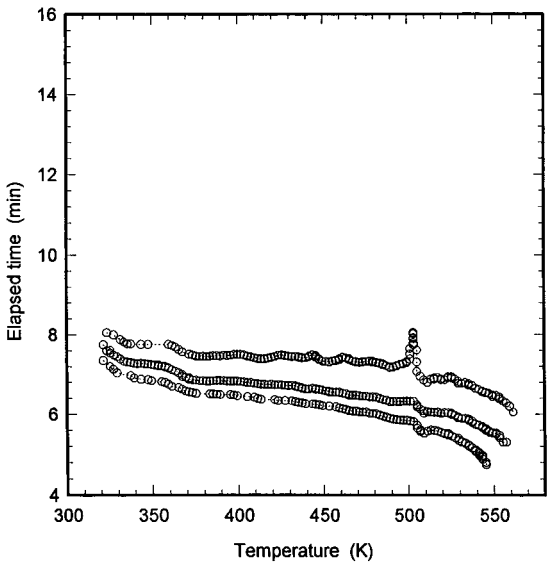

Figure 5. Same as Figure 4 on cooling.

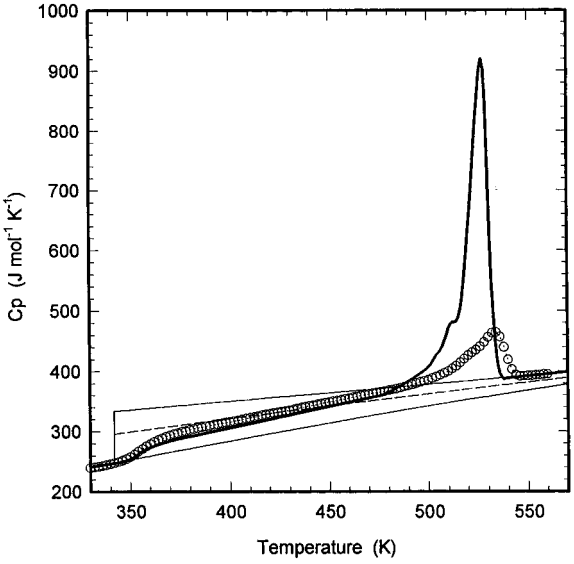

Figure 6. Heat capacity by standard DSC (thick line) and reversing heat capacity by quasi-isothermal TMDSC (open circles). Both on the same melt-crystallized PET. The thin lines indicate the Data Bank data for the amorphous and crystalline PET; the broken line indicates the computed heat capacity for 44% crystalline PET.

The reversing heat capacity for the biaxially oriented PET film by the quasi-isothermal measurement is shown in Figure 11 (filled circles). As before, the reversing heat capacity of Figure 6 is shown for comparison by the open circles. The glass transition occurs at a considerably higher temperature and indicates a larger fraction of rigid amorphous component.[21] The integral value for the PET film above the baseline is 1.88 kJ/mol; i.e., the reversing crystallinity is 7.0%, compared with the total crystallinity of 42% measured by standard DSC.

Discussion

Separation of Irreversible and Reversing Effects. It is by now well-known that TMDSC can

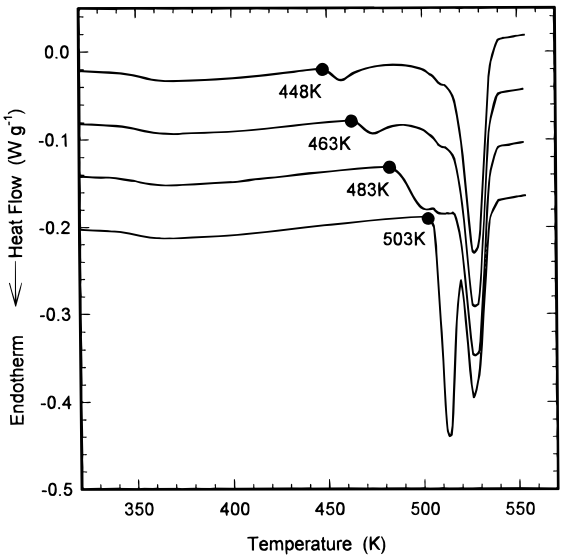

Figure 7. Standard DSC heat-flow signals after the quasi-isothermal measurement at the temperature which is marked in the figure. After the TMDSC the samples were quickly cooled before heating from 250 K to 560 K at 10 K/min.

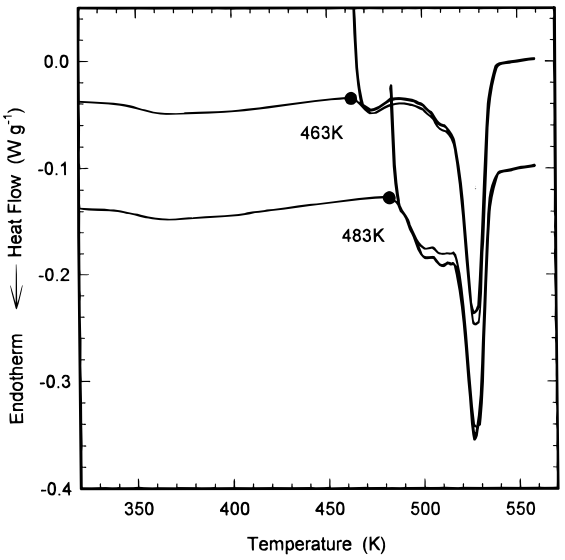

Figure 8. Same as Figure 7. The thick lines are for DSC experiments that followed the TMDSC without cooling after the quasi-isothermal experiment.

separate rather large irreversible effects such as the enthalpy relaxation at the glass transition, the heat of chemical reaction, and the heat of fusion on cold crystallization from the reversing heat capacity contributions. Using rather slow underlying heating rates or quasi-isothermal heating, the frequency dependence of the apparent heat capacities of poly(ethylene terephthalate)[21,22] and polystyrene[22] in the glass-transition region were analyzed quantitatively; the heat capacity of the fullerene C_{70} was checked in the presence of slow oxidation up to 700 K;[23] the progress of curing of epoxies was checked by measurement of the reversing heat capacity in the glass transition region during the reaction;[24] and most recently, the kinetics of crystallization of polyethylene was evaluated from the change in heat capacity in the presence of the heat of crystallization.[25] In addition, qualitative techniques for identification of exotherms in the presence of endotherms have been described.[26] The study of melting transitions of sharply melting substances is more difficult because of limits set to maintain steady state.[27] For indium, as

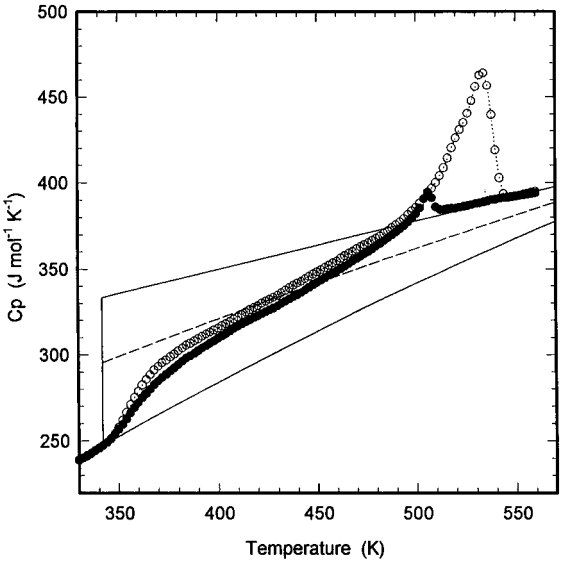

Figure 9. Reversing heat capacity by quasi-isothermal TMDSC on cooling from the melt (filled circles). The thin lines indicate the Data Bank data for the amorphous and crystalline PET; the broken line indicates the computed heat capacity for 49% crystalline PET. The open circles are melt-crystallized PET of Figure 6 on the quasi-isothermal upon step-heating as reference.

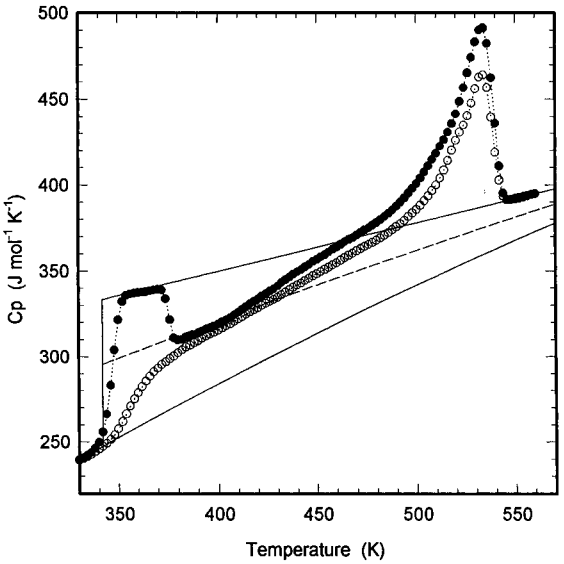

Figure 10. Reversing heat capacity by quasi-isothermal TMDSC on heating of a quenched, amorphous sample (filled circles). The thin lines indicate the Data Bank data for the amorphous and crystalline PET; the broken line indicates the computed heat capacity for 40% crystalline PET. The open circles are melt-crystallized PET of Figure 6 on the quasi-isothermal upon step-heating as reference.

an example, rather small sample masses had to be used and the melting effect had to be separated from the heat capacity by mathematical curve fitting.[28] In the present case, the melting range is broad, mainly caused by a distribution of crystals of different degrees of metastability,[2] and the quasi-isothermal analysis can be extended, if needed, to many hours to reach steady state, as shown in Figure 2. This new method opens, thus, the possibility to get more insight into the multitude of processes expected on melting of macromolecules.

Melting/Crystallization Kinetics and Molecular Nucleation. A comparison of melting and crystallization kinetics of crystals which produce small molecules and macromolecular crystals which maintain molecular integrity has shown that only when small molecules

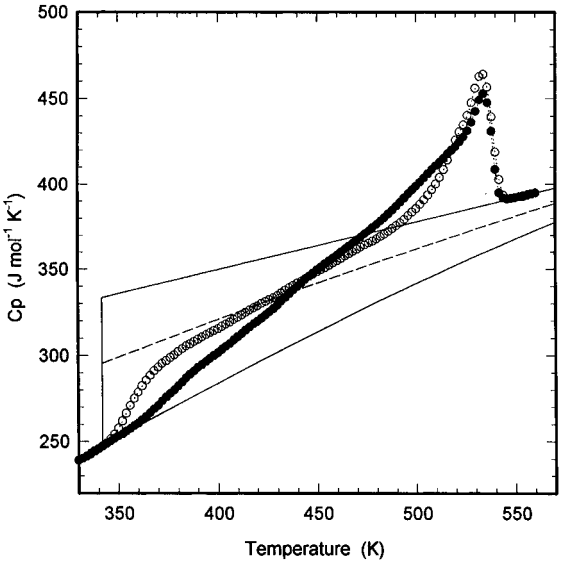

Figure 11. Reversing heat capacity by quasi-isothermal TMDSC on heating for the biaxially drawn PET film (filled circles). The thin lines indicate the Data Bank data for the amorphous and crystalline PET; the broken line indicates the computed heat capacity for 42% crystalline PET. The open circles are melt-crystallized PET of Figure 6 on the quasi-isothermal upon step-heating as reference.

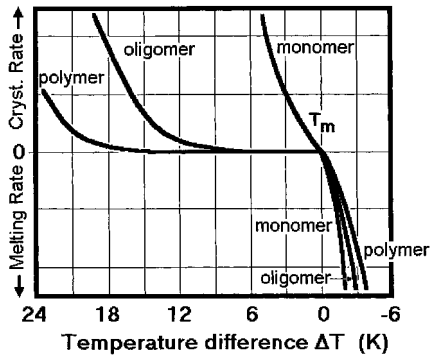

Figure 12. Schematic of the melting and crystallization rates as a function of supercooling and superheating. The equilibrium melting temperature is T_m.

exist in the melt in the presence of crystal nuclei are melting and crystallization continuous through the melting point.[29] A condition for this continuity is the presence of a quasi-crystalline melt.[5] Figure 12 shows a schematic of melting and crystallization rates patterned after experiments of melting and crystallization kinetics of various substances.[2,30] The monomer crystallization and melting rates show continuity through the melting temperature, T_m. The curve is drawn according to data collected for GeO_2,[2,31] P_2O_5,[2,32] and the crystallization of Se_2 from the gas phase[29,33] and according to the extrapolation of data on poly(oxyethylene) to the monomer mass.[34] The oligomer melting and crystallization curve is similar to data for poly(oxyethylene) of molar mass 6000 Da.[35] The polymer curves are drawn as seen for data on polyethylene,[2,30,36] selenium melt,[37,38] poly(oxyethylene),[34,35] poly(oxymethylene),[39,40] poly(tetrafluoroethylene),[40,41] and polycaprolactam.[42] In all cases it is seen that the greater the anticrystalline character, the bigger is the region of metastability of the polymer melt below T_m. In this temperature region crystal nucleation cannot break the metastability, as was demonstrated by calorimetry of polyethylene melt seeded with extended chain crystals.[43] The reason for the temperature range of metastability is the need for a melted molecule to undergo molecular nucleation before crystallization.[7,8] The need for molecular nucleation also supplies the reason for the high efficiency of segregation of molecular masses on crystallization *below* the equilibrium or zero-entropy-production melting temperature of the rejected species.[8,34,44]

Reversible Melting. Quasi-isothermal TMDSC in the melting range should, according to Figure 12, have no contribution to the reversing heat capacity. Figures 6 and 9−11 show, however, that this is not so. A reversing contribution to the heat capacity is present and depends on the crystallization conditions. Although the contribution is much less than that of the total heat of fusion, the reversing contribution is not negligible. The only interpretation of this observation is that the polymer molecules that contribute to the reversing heat capacity are still attached to crystals that melt at a higher temperature and can serve as molecular nuclei. After the heating cycle there is, thus, a number of melted polymer molecules that are still attached to higher melting crystals and can recrystallize during the cooling cycle with negligible supercooling. Overall, this process yields a reversible, apparent heat capacity contribution.

Fractions of attached molecules were discovered some 20 years ago as nonextractable, melted polyethylene.[45] After partial melting, the samples of polyethylene were quenched, so that the melted molecules or parts of molecules would recrystallize to poorer, lower-melting crystals. The crystals from the fully melted molecules could then be extracted with a suitable solvent at or below the dissolution temperature that is equivalent to the original melting temperature. The attached molecules could not be extracted. They could, however, be identified by renewed thermal analysis as a low melting portion. The TMDSC analysis gives now a quantitative accounting for the attached molecules that locally melt and crystallize reversibly.

Although it looks on initial inspection that steady state was reached for all temperatures after 20 min, Figure 2b indicates that the attached molecules decrease slowly in number. Continued very slow irreversible melting takes place. Present estimates suggest that at the chosen 522 K experiment it may take some 20 h to reach negligible reversible melting. This observation points to the problem of interpretation of TMDSC and the opportunity to gain additional, quantitative information about the melting process. New experiments are planned to reveal more about the kinetics and mechanism of melting.

Influence of Morphology on the Melting Characteristics. Taking the melt-crystallized PET as a reference substance, one can see from Figure 9 that on slow cooling no crystallization occurs until about 510 K (supercooling of about 40 K relative to the equilibrium melting temperature, 553 K, and 30 K relative to the end of melting of Figure 6). Then a sample is crystallized that behaves similar to the normal melt-crystallized PET, but with somewhat higher crystallinity (lower heat capacity above the glass transition).

Cold crystallization, seen in Figure 9 leads to somewhat lower crystallinity. The crystallization is fully irreversible but does not complete in one temperature step. The poorer crystals expected on cold crystallization lead to a larger amount of locally reversible melting over the whole melting range. The biaxially drawn sample, in contrast, has more locally reversible melting occurring for low melting crystals, and less for high melting crystals.

Glass Transition and Rigid Amorphous Fraction. Details about the glass transition that can be

gained by TMDSC were discussed earlier on a wide range of samples of different degrees of crystallinity and orientation.[21] The data of Figures 6 and 9−11 match the earlier data which were used to evaluate the broadening of the glass transitions, their activation energies and the preexponential factors. A question that could not be discussed earlier is the change in rigid amorphous fraction with temperature. The rigid-amorphous fraction is the part of the noncrystalline PET that does not participate in the measured ΔC_p at the glass transition but, on the other hand, does also not contribute to the heat of fusion.[46,47] The figures show that the reversing heat capacities reach the expected equilibrium heat capacity of the semicrystalline PET derived from the data bank[16] at about 430 to 450 K. Unfortunately, this temperature is sufficiently close to the beginning of melting that the actual crossover temperature may be somewhat higher due to some low-temperature reversible melting. Checking Figure 10, it looks like the cold crystallized polymer has only a small rigid-amorphous fraction and starts melting at about 410 K. This may be an indication that the rigid-amorphous fraction in the other samples may tend, indeed, to zero at the beginning of the fusion process. More quantitative answers may come from long-time quasi-isothermal experiments, presently in the planning stage.

Acknowledgment. This work was financially supported by the Division of Materials Research, NSF, Polymers Program, Grant No. DMR 90-00520 and Oak Ridge National Laboratory, managed by Lockheed Martin Energy Research Corp. for the U.S. Department of Energy, under contract number DE-AC05-96OR22464. Support for instrumentation came from TA Instruments, Inc. Research support was also given by ICI Paints and Toray Industries, Inc.

References and Notes

(1) Stuart, H. A., Ed. *Die Physik der Hochpolymeren*; Springer Verlag: Berlin and New York, 1955; Vol. 3, Sections 35−49.
(2) Wunderlich, B. Macromolecular Physics*; Crystal Nucleation, Growth, Annealing* (Vol. 2) and *Crystal Melting* (Vol. 3); Academic Press: New York, 1980.
(3) Proceedings and discussions published in: *Discuss. Faraday. Soc.*, **1979**, *68*.
(4) Proceedings of the NATO Advanced Research Workshop on Crystallization of Polymers, Mons, Sept 7−11, 1992. Published in: Dosiére, M. Ed. *Crystallization of Polymers*; NATO ASI Series, C, Volume 405; Kluver Academic Publishers: Dordrecht, The Netherlands, 1993.
(5) Ubbelohde, A. R. *Melting and Crystal Structure*, Clarendon Press: Oxford, U.K., 1965.
(6) Flory, P. J. *Statistical Mechanics of Chain Molecules*; Interscience Publishers: New York, 1969.
(7) Wunderlich, B.; Mehta, A. *J. Polym. Sci., Polym. Phys. Ed.*, **1974**, *12*, 255.
(8) Mehta, A.; Wunderlich, B. *Colloid Polym. Sci.*, **1975**, *253*, 193.
(9) Reading, M.; Elliot, D.; Hill, V. L. *J. Thermal Anal.* **1993**, *40*, 949.
(10) Gill, P. S.; Sauerbrunn, S. R.; Reading, M. *J. Thermal Anal.* **1993**, *40***,** 931.
(11) Reading, M. *Trends Polym. Sci.* **1993**, *8***,** 248.
(12) Wunderlich, B.; Jin, Y.; Boller, A. *Thermochim. Acta* **1994**, *238*, 277.
(13) Wunderlich, B. *Thermal Analysis*; Academic Press: Boston, MA, 1990.
(14) Wunderlich, B.; Boller, A.; Okazaki, I.; Kreitmeier, S. *Thermochim. Acta.* **1996**, *282/283*, 143.
(15) Boller, A.; Jin, Y.; Wunderlich, B. *J. Thermal Anal.* **1994**, *42*, 307.
(16) See WWW (Internet), URL: http://funnelweb.utcc.utk.edu/~athas. For a general description see also: Wunderlich, B. *Pure Appl. Chem.* **1995**, *67*, 1919.
(17) Ozawa, T.; Kanari, K. *Thermochim. Acta* **1995**, *253*, 183.
(18) Zero-entropy-production melting refers either to equilibrium melting or to melting of a metastable crystal to a melt of identical metastability. First proposed for the description of polymer melting by Wunderlich, B. *Polymer* **1964**, *5*, 611.
(19) Ditmars, D. A.; Ishihara, S.; Chang, S. S.; Bernstein, G.; West, E. D. *J. S. Res. Natl. Bur. Stand.* **1982**, *87*, 159.
(20) Wunderlich, B. To be published in *J. Thermal Anal.*
(21) Okazaki, I.; Wunderlich, B. *J. Polym. Sci., Part B: Polym. Phys.* **1996**, *34*, 2941.
(22) Wunderlich, B.; Boller, A.; Okazaki, I.; Kreitmeier, S. *J. Thermal Anal.* **1996**, *47*, 1013.
(23) Jin, Y.; Xenopoulos, A.; Cheng, J.; Chen, W.; Wunderlich, B.; Diack, M.; Jin, C.; Hettich, R. L.; Compton, R. N.; Guiochon, G. *Mol. Cryst. Liq. Cryst.* **1994**. *257*, 235−250.
(24) Van Assche, A.; Van Hemelrijck, A.; Rahier, H.; Van Mele, B. *Thermochim. Acta* **1995**, *268*, 121.
(25) Toda, A.; Oda, T.; Hikosaka, M.; Daruyama, Y. *Thermochim. Acta*, to be published.
(26) TA Instruments, Application Notes. Available from TA Instruments, Inc., 109 Lukens Drive, New Castle, DE 19720.
(27) Ozawa, K.; Kanari, K. *J. Thermal Anal.*, to be published.
(28) Isikiriyama, K.; Boller, A.; Zhang, G.; Okazaki, I.; Wunderlich, B. *J. Thermal Anal.* to be published.
(29) Wunderlich, B. *Discuss. Faraday. Soc.* **1979**, *68*, 239.
(30) The first description of superheating and melting kinetics of macromolecules was given by Hellmuth, E.; Wunderlich, B. *J. Appl. Phys.* **1965**, *36*, 3039.
(31) Vergano, P. J.; Uhlmann, D. R. *Phys. Chem. Glasses* **1970**, *11* 30, 39.
(32) Cormia, R. L.; Mackenzie, J. D.; Turnbull, D. *J. Appl. Phys.* **1963**, *34*, 2239.
(33) Shu, H.-C.; Wunderlich, B. *Polymer*, **1980**, *21*, 521.
(34) Cheng, S. Z. D.; Wunderlich, B. *J. Polym. Sci., Part B: Polym. Phys.* **1986**, *24*, 577, 595.
(35) Kovacs, A. J.; Straupe; Gonthier, A. *J. Polym. Sci., Polym. Symp.* **1975**, *50*, 383.
(36) Mandelkern, L. *SPE J.* **1959**, *15*, 63.
(37) Wunderlich, B.; Shu, H.-C. The Crystallization and Melting of Selenium. *J. Cryst. Growth* **1980**, *48*, 227.
(38) Crystal, R. G. *J. Polym. Sci., Polym. Phys. Ed.* **1970**, *8*, 2153.
(39) Jaffe, M.; Wunderlich, B. *Kolloid Z. Z. Polym.* **1967**, *216−217*, 203.
(40) Wunderlich, B. *Kolloid Z. Z. Polym.* **1969**, *231*, 605.
(41) Hellmuth, E.; Wunderlich B.; Rankin, J. M. *Appl. Polym. Symp.* **1966**, *2*, 101.
(42) Liberti, F. N.; Wunderlich, B. *J. Polym. Sci., Polym. Phys. Ed.* **1968**, *6*, 833.
(43) Wunderlich, B.; Cormier, C. M. *J. Phys. Chem.* **1966**, *70*, 1844.
(44) Cheng, S. Z. D.; Bu, H. S.; Wunderlich, B. *J. Polym. Sci., Part B: Polym. Phys.* **1988**, *26*, 1947.
(45) Mehta, A.; Wunderlich, B. *Makromol. Chem.* **1974**, *175*, 977.
(46) Suzuki, H.; Grebowicz, J.; Wunderlich, B. *Br. Polym. J.* **1985**, *17*, 1.
(47) For a general discussion of glass transitions in semicrystalline polymers see, for example: Wunderlich, B. *Colloid Polym. Sci.* **1994**, *96*, 22.

MA961539D